The Cryosphere

Open Access

What drives basin scale spatial variability of snowpack properties in northern Colorado?

G. A. Sexstone and S. R. Fassnacht

ESS-Watershed Science Program, Warner College of Natural Resources, Colorado State University, Fort Collins, Colorado 80523-1476, USA

Correspondence to: G. A. Sexstone (graham.sexstone@colostate.edu)

Abstract. This study uses a combination of field measurements and Natural Resource Conservation Service (NRCS) operational snow data to understand the drivers of snow density and snow water equivalent (SWE) variability at the basin scale (100s to 1000s km^2). Historic snow course snowpack density observations were analyzed within a multiple linear regression snow density model to estimate SWE directly from snow depth measurements. Snow surveys were completed on or about 1 April 2011 and 2012 and combined with NRCS operational measurements to investigate the spatial variability of SWE near peak snow accumulation. Bivariate relations and multiple linear regression models were developed to understand the relation of snow density and SWE with terrain variables (derived using a geographic information system (GIS)). Snow density variability was best explained by day of year, snow depth, UTM Easting, and elevation. Calculation of SWE directly from snow depth measurement using the snow density model has strong statistical performance, and model validation suggests the model is transferable to independent data within the bounds of the original data set. This pathway of estimating SWE directly from snow depth measurement is useful when evaluating snowpack properties at the basin scale, where many time-consuming measurements of SWE are often not feasible. A comparison with a previously developed snow density model shows that calibrating a snow density model to a specific basin can provide improvement of SWE estimation at this scale, and should be considered for future basin scale analyses. During both water year (WY) 2011 and 2012, elevation and location (UTM Easting and/or UTM Northing) were the most important SWE model variables, suggesting that orographic precipitation and storm track patterns are likely driving basin scale SWE variability. Terrain curvature was also shown to be an important variable, but to a lesser extent at the scale of interest.

1 Introduction

A majority of earth's moving freshwater originates in snow-dominated mountainous areas (Viviroli et al., 2003), with 60 to 75 percent of annual streamflow in the Rocky Mountain region of the western United States originating from snowmelt (Doesken and Judson, 1996). A comprehensive understanding of the distribution of the seasonal mountain snowpack and estimation of its snow water equivalent (SWE) is essential to improve hydrologic models used for forecasting water availability. Additionally, the recent shift towards earlier snowmelt in regions of the western US (e.g., Stewart, 2009; Clow, 2010) necessitates a more accurate accounting for future water resources planning. Mountainous landscapes have complex topography as well as strong and highly variable climatic gradients, yielding spatial and temporal (seasonal and interannual) variability in snowpack properties. Determining the meteorology and related feedbacks that drive hydrologic processes in these areas is challenging, as the resolution of available SWE measurements is often much coarser than the scale needed to characterize the correlation length of its spatial variability (Blöschl, 1999), and requires spatial scaling (Bales et al., 2006).

Across the western US, the Natural Resource Conservation Service (NRCS) SNOwpack TELemetry (SNOTEL) and snow course network provide operational snowpack measurements of snow depth and SWE from which snow density

can be calculated at a daily and monthly time step, respectively. Hourly SNOTEL data are also available, but were not used in this study. NRCS operational stations were established to measure the snowpack for water supply forecasts, yet, they have been shown to represent SWE only as a point location rather than surrounding area (Molotch and Bales, 2005). Nonetheless, SNOTEL and snow course sites are the most widely available and utilized ground-based measurements of SWE and relied upon heavily for estimating basin scale snow distribution.

Research on the spatial distribution of snow has emphasized the statistical relation between snow properties and terrain characteristics, the latter as a surrogate for the driving meteorology. These studies have used SNOTEL data to interpolate SWE over large basins (e.g., Fassnacht et al., 2003), as well as manual field snowpack measurements over small catchments (e.g., Elder et al., 1991). However, few studies have analyzed snow's spatial variability at the basin scale using both operational and field-based measurements. Operational measurements can provide regional knowledge on the spatial distribution of snow (e.g., Fassnacht et al., 2003), yet cannot accurately characterize the basin scale variability that vitally impacts snowmelt and runoff (Bales et al., 2006). It has been recommended that future research should focus on more accurate estimation of SWE at the basin (100s to 1000s km^2) and regional (10 000s to 100 000s km^2) scale to effectively assess and manage mountain water resources (Viviroli et al., 2011). There is a need to supplement operational data with additional field-based snowpack measurements at this scale of interest to evaluate the spatial variability of SWE and provide additional ground-truth measurements within the scale extent of remote sensing observations. At the basin scale, an approach to reducing the sampling effort is to use snow depth as a surrogate for SWE by developing a model for snow density, as manual snow density measurements require more time and effort than snow depth measurements. Recent studies have attempted to characterize the spatiotemporal characteristics of snow density (e.g., Mizukami and Perica, 2008; Fassnacht et al., 2010), or to develop reliable methods for modeling snow density and thus estimating SWE from snow depth measurements (e.g., Jonas et al., 2009; Sturm et al., 2010).

The objectives of this research were (1) to evaluate basin scale snow density variability from historic snow course measurements and develop a snow density model specific to our study area that can be used to estimate SWE from snow depth measurements; this is a different domain and scale than used in previous studies, and (2) to combine operational SNOTEL and snow course measurements, as suggested by Dressler et al. (2006), with supporting field-based snowpack measurements to evaluate what is driving variability of the snowpack at the basin scale.

2 Study area and datasets

This study was conducted in the Cache la Poudre Basin located in the Front Range of northern Colorado and a small portion of southeastern Wyoming (Fig. 1). We focus on the portion of this basin that shows persistent snow cover near peak snow accumulation; this region is responsible for the majority of hydrologic input to the river system. To define this area, we use the Snow Cover Index (SCI) at 50 % (Richer et al., 2013), which represents the area that was snow-covered at least 50 % of the time from 2000 to 2010 during early April. The SCI is calculated based on the Moderate Resolution Imaging Spectroradiometer (MODIS)/Terra 8-day snow cover products. The portion of the basin within the 50 % SCI has an area of 1493 km^2 and ranges in elevation from 2040 to 4125 m. Spruce-fir (*Picea engelmannii* and *Abies lasiocarpa*), lodgepole pine (*Pinus contorta*), and ponderosa pine (*Pinus ponderosa*) forests cover a majority (approximately 77 %) of this area, with the alpine community located at the highest elevations and the mountain shrub community located at the lowest elevations. Snow is the dominant form of precipitation within the basin, and the hydrograph peak is driven by snowmelt generally occurring in late May to June. The majority of winter moisture moves into this region by Pacific frontal storm tracks from the west, southwest, or northwest, however, systems moving north from the Gulf of Mexico can also bring substantial snowfall to the Front Range of Colorado (Barry, 2008).

The NRCS operational stations located within the study area and in a 15 km buffer around the basin were analyzed (Fig. 1), yielding a total of 10 SNOTEL stations and 17 snow courses. Deadman Hill and Joe Wright, the two long-term SNOTEL stations located within the Cache la Poudre Basin, have a mean (1980 to 2012) peak SWE of 538 mm and 690 mm, respectively (Fig. 2). The lowest snow year recorded was 2002 at Deadman Hill and 2012 at Joe Wright, while the maximum snow year was 2011 at both SNOTEL stations. Despite the similar elevation of the two stations, historically Joe Wright (3085 m) has a greater accumulation of snow than Deadman Hill (3115 m).

Field snow surveys were conducted on and about 1 April 2011 and 2012 within the study area. At each field sampling location, snow density (ρ_s) and/or snow depth (d_s) measurements were taken and Universal Transverse Mercator (UTM) geographic coordinates were recorded using a global positioning system (GPS). In order to account for small-scale spatial variability at each location (e.g., López-Moreno et al., 2011), snow depths were sampled at 1 m intervals along 10 m transects in one of the four cardinal directions. Snow density is a conservative variable that varies less spatially than depth (Logan, 1973; Fassnacht et al., 2010), thus, fewer snowpack density measurements were made across the study area than depth. Three methods of measuring snow density were used at each site. A cylindrical metal can with a diameter of 15.3 cm was used to measure snow density if the
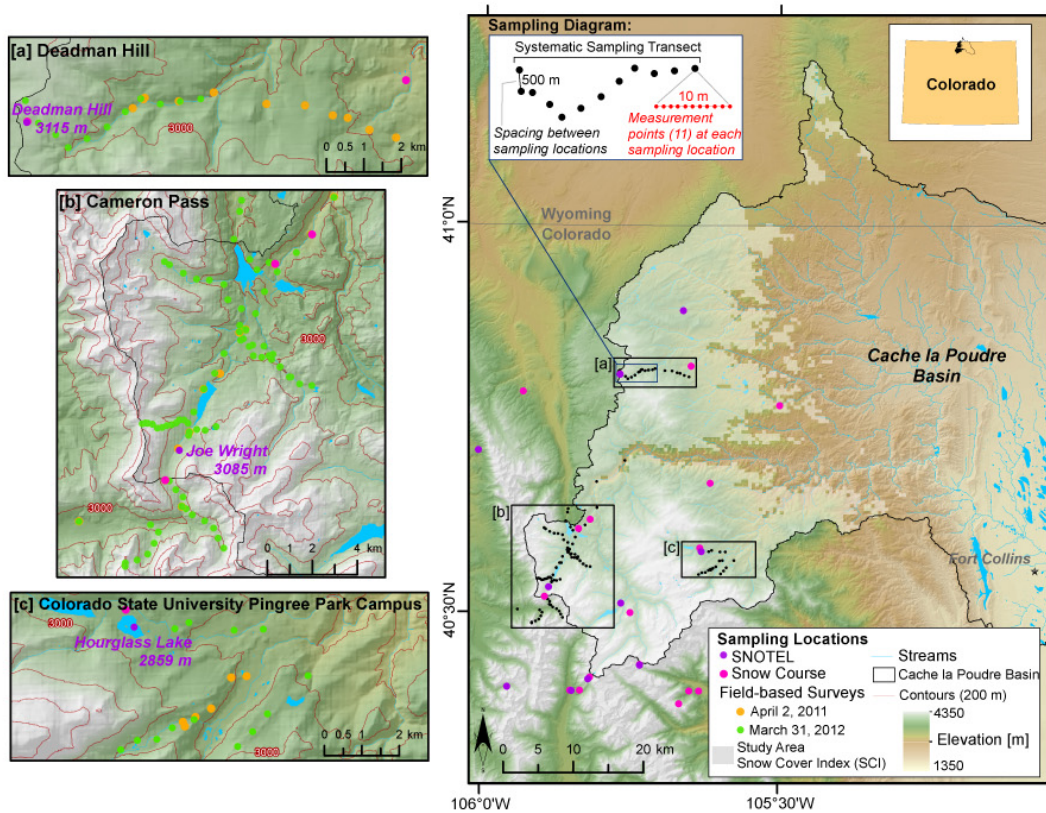
Fig. 1. The Cache la Poudre Basin located in the northern Front Range of Colorado, USA. The study area is represented by the 50 % Snow Cover Index (SCI) which is indicated by the transparent light gray color within the basin. The locations of operational and field-based snow measurements are shown, including a detailed sampling diagram of one systematic field-based sampling transect.
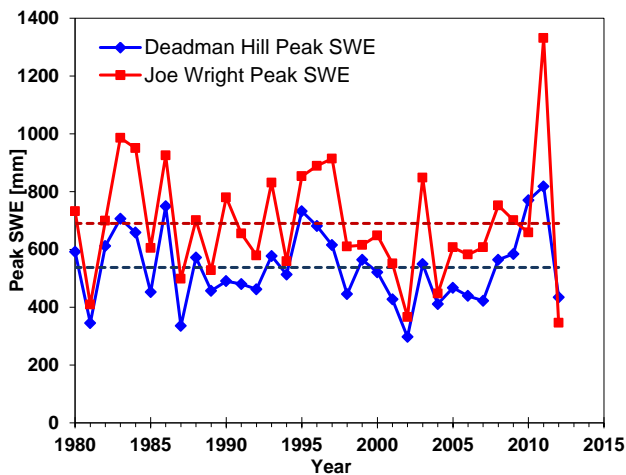

Fig. 2. Annual peak SWE and mean annual peak SWE (1980 to 2012) for Deadman Hill and Joe Wright SNOTEL stations.

snowpack was less than 50 cm. A cylindrical plastic snow sampling tube with a diameter of 6.6 cm was used to measure snow density for snowpacks greater than 50 cm and less than 150 cm. Additionally, a Federal Sampler (diameter of 3.77 cm) was used to measure the snow density for snowpacks greater than 150 cm, but it was also used at some locations shallower than 150 cm. Each of the field-based surveys included transects of sampling locations with a systematic spacing of approximately 500 m (Fig. 1). A total of 28 field sampling locations, including 11 ρ_s measurements, were monitored on and about 1 April 2011 and 104 field sampling locations, including 12 ρ_s measurements, on and about 01 April 2012. The location of snow survey transects were selected based on accessibility as well as representation of snow-producing regions within the study area. The high-elevation areas located around the Colorado State University Pingree Park Campus, Cameron Pass, and Deadman Hill were the focus within the Cache la Poudre Basin (Fig. 1).

The 2011 field-based snow survey was completed over the span of three days (31 March through 2 April 2011), while the 2012 survey was completed over four days (29 March through 1 April 2012). Small amounts of precipitation was recorded at SNOTEL stations within the study area during the 2011 and 2012 survey time period, however the majority of change to the snowpack during these periods were due to melt, compaction, and/or metamorphism. Changes in snow depth were accounted for using daily SNOTEL snow depth

measurements to standardize the field-based snow depth measurements to a single date for each survey. The average change in snow depth among SNOTEL stations was added to our field-based snow depth measurements outside of the standardized date to adjust for the change in snow depth over that period. Snow depth measurements from the 2011 survey were standardized to 2 April, while 2012 measurements were standardized to 31 March.

3 Background and methods

3.1 Snow density model

SWE, in millimeters, is the product of snow depth (d_s) measured in meters and snow density (ρ_s) in kilograms per cubic meter. At operational sites, the seasonal variability of snow density is largely dictated by time of year, and interannual variability is typically low (Mizukami and Perica, 2008). However, previous spatial snow surveys have shown that snow density can exhibit inter-annual variability, particularly in continental regions (e.g., Balk and Elder, 2000; Jepsen et al., 2012). Snow density tends to increase gradually throughout the snow season due to crystal metamorphism, settling, and compaction. Therefore, snow density tends to increase with the day of year (Mizukami and Perica, 2008) and with increasing snow depth (Pomeroy and Gray, 1995). Elevation has also been shown to influence snow density, with the effect often being dependent on the day of year (e.g., Jonas et al., 2009). Topography and tree canopy also impact snow densification, as they can be surrogates for solar radiation. However, large datasets of snow density are rare, and not often meant to represent varying terrain and canopy conditions, which limits the ability of these data to represent the variability explained by those variables. Since the range of variability of snow density is more conservative than snow depth and SWE (e.g., Logan, 1973; Fassnacht et al., 2010), estimating density from depth has been shown to provide a reasonable pathway for estimating SWE from a snow depth measurement. Based on the approaches presented by Jonas et al. (2009) and Sturm et al. (2010) we have analyzed historic operational snow density data for the Cache la Poudre Basin to develop and evaluate a snow density model. We acknowledge that the operational snow density data evaluated are not representative of potential terrain and canopy controls on the variability of snow density at the basin scale. However, the potential drivers of snow depth, time of year, elevation, and region are adequately represented. The development of this type of model provides a mechanism for estimating SWE from snow depth, and also may provide insights into regional tendencies of snow density variability not accounted for in these prior models.

Historical data from 17 NRCS snow courses (1936 to 2010, $n = 3637$; Fig. 1) were evaluated. These snow courses range in elevation from 2408 m to 3261 m and are (generally)

measured on or about the first of the month from January through June each year. Snow course measurements consist of the average of approximately ten measurements that are made with a Federal Sampler. For the analysis, snow density values greater than $600 \, \text{kg m}^{-3}$ and less than $50 \, \text{kg m}^{-3}$ were omitted. Additionally, due to the limited precision and possibly the lack of accuracy for snow density measurements in shallow snowpacks, data for snow depth less than 0.13 m and/or SWE less than 50 mm were also omitted. This selection of data resulted in 3262 data records of snow depth, snow density, and SWE, with 10.3 % of the original data being removed.

A multiple linear regression model was developed to predict snow density considering snow depth (d_s), Julian day (DOY), elevation (z), UTM Easting (UTM_e), and UTM Northing (UTM_n) as independent variables. The statistical software R (R Development Core Team, 2012) was used for all statistical analyses. The final independent variables included in the multiple linear regression model were selected based on an all-subsets regression procedure (Berk, 1978), which assesses a criterion statistic for every possible combination of independent variables. Mallows' C_p (Mallows, 1973), which assesses the fit of a regression model and increases a penalty term as the number of predictor variables increases, was used as a criterion for the all-subsets regression. Additionally, a criterion was set so that all predictor variables included were required to be statistically significant within the model ($p < 0.05$). Candidate models that showed the best Mallows' C_p values were then evaluated using the Akaike information criterion (AIC) statistic (Akaike, 1974), which is also a measure of the relative goodness of fit of the statistical model that introduces a penalty for increasing the number of model parameters. The variance inflation factor (VIF) was used to quantify the severity of multicollinearity between independent variables. A VIF score greater than 4 may suggest multicollinearity between variables (Kutner et al., 2005). Model diagnostics were evaluated using residual plots to check the model assumptions of normality, linearity, and homoscedasticity and were used to determine if variable transformations were necessary. Final model selection was based on the results of criterion statistics and model diagnostics (Kutner et al., 2005). Also, if an effort to ensure our model was physically robust, independent variables were only included within the model if their coefficients made physical sense.

The multiple regression model provides an estimate of snow density for each snow depth measurement and their product yields an estimate of SWE. To assess the accuracy of the snow density model, several methods of model evaluation were performed. Calibration was performed by comparing modeled snow density as well as calculated SWE with observed values from the original data set; explained variance was computed. Model validation with two sets of independent data was also completed to test model transferability to predict independent data. The two independent datasets

included monthly (January through May) field-based measurements from the 2011 and 2012 snow seasons ($n = 84$), as well as historic first of the month SNOTEL measurements ($n = 121$) at sites that are not co-located with a snow course. The monthly field-based snow density measurements not collected about 1 April were only used for model validation within this study. Performance of the final snow density model was determined from the residuals of both observed snow density as well as calculated SWE through the calculation of the coefficient of determination (R^2) and root mean squared error (RMSE) performance statistics.

3.2 Basin scale SWE variability

Topographic variables that are thought to potentially drive the spatial distribution of snow at the scale of interest were derived from a 30 m-resolution digital elevation model (DEM) of the study area. The DEM was downloaded from the USGS National Elevation Dataset (NED) (http://ned.usgs.gov). A value of the derived terrain variables (spatial data grids) was extracted for each sampling location based on its corresponding 30 m DEM pixel. A description of the derivation and importance of each of the spatial data grids is provided below.

Location within the study area is represented by UTM Zone 13N Easting and Northing coordinates for each operational and field-based sampling location. A 30 m-resolution spatial data grid of UTM Easting and Northing was created for the study area in ArcGIS (ESRI, 2011) by assigning the mean UTM value to each pixel. Spatially continuous coordinates of UTM Easting and Northing can be correlated with the distribution of snow in various ways that depend on site location and scale. Previous studies have used distance to a mountain barrier and distance to ocean or source of moisture (e.g., Fassnacht et al., 2003; López-Moreno and Nogués-Bravo, 2006), which can also be represented by UTM Easting for the study site due to its geographic orientation. Furthermore, given the scale of the study, UTM Easting and Northing represent different regions within the study area that are thought to display different patterns of snow accumulation and ablation due to the variability of meteorology and storm tracks.

Elevation was extracted for each sampling location directly from the 30 m DEM. Snow accumulation has long been shown to be a function of elevation (e.g., Washichak and McAndrew, 1967; Dingman, 1981) due to orographic precipitation patterns and the effect of air temperature (Doesken and Judson, 1996).

Slope was derived from the 30 m DEM using the Spatial Analyst tools within ArcGIS to provide an output spatial data grid with a value of slope (in degrees) for each pixel. The degree of slope impacts the stability of the snowpack (influencing snow accumulation and redistribution) and input of solar radiation (influencing melt) (Anderton et al., 2004). Previous studies have used slope angle as an explanatory variable for

describing the distribution of snow (e.g., Kerr et al., 2013), therefore the variable was tested in this study.

Aspect (in degrees) was also derived from the 30 m DEM using the Spatial Analyst tools within ArcGIS. Aspect can be problematic as an independent variable due to its continuous range of 0 to 360°, thus normalizing this variable is necessary. Degrees of northness and eastness were calculated to normalize the aspect variable (Fassnacht et al., 2001; Fassnacht et al., 2012). Degree of northness is the product of the cosine of aspect and the sine of slope (Molotch et al., 2005), while degree of eastness is the product of the sine of aspect and the sine of slope. Northness is a measure of the degree that terrain is north facing, therefore we would expect SWE to show a positive correlation with northness as snow tends to be more persistent on north facing slopes. Similarly, eastness is a measure of the degree that terrain is east facing. Within our study area, we expect eastness to show a positive correlation with SWE as east-facing slopes are most often the leeward side of dominant west winds and can receive snow loading from windward slopes. Exposure of slope aspect controls solar radiation input, which influences snowpack stability, densification, and ablation (McClung and Schaerer, 2006).

Solar radiation was derived using the Area Solar Radiation tool in ArcGIS, which calculates incoming solar radiation across a DEM surface for a specified time interval. Given the latitude of the study area, the average clear-sky solar radiation (in W m^{-2}) from 15 November through 30 March was calculated for each pixel. Cumulative incoming solar radiation is calculated based on solar zenith angle and terrain shading, and does not consider the influence of forest canopy. Previous studies have successfully used solar radiation spatial data grids derived by similar methods within statistical models describing the distribution of snow (e.g., Elder et al., 1998; Anderton et al., 2004; Erickson et al., 2005).

Terrain curvature was derived from the 30 m DEM using the Spatial Analyst tools within ArcGIS to provide an output spatial data grid with a value of curvature for each pixel. Terrain curvature is defined as the second derivative of the surface (Kimerling et al., 2011). Terrain curvature, referred to as curvature in this study, is a combination of profile and planform curvature. This variable represents the local relief of terrain (i.e., concavity or convexity) in all directions, which, in terms of snow accumulation, primarily accounts for wind drifting from high-exposure areas with steep slopes to low-lying gullies (Blöschl et al., 1991; Lapen and Martz, 1996). Curvature was calculated using both 30 m DEM resolution (90 m footprint) and 100 m DEM resolution (300 m footprint) and will be referred to as curvature 30 and curvature 100, respectively. Negative curvature values represent concave surfaces, thus we expect curvature and SWE to show a negative correlation due to local snow loading within concave-positioned areas.

Maximum upwind slope (Winstral et al., 2002) is a terrain-based variable that has been shown to account for redistribution of snow by wind, which is especially important in alpine

areas. However, this variable requires the knowledge of predominant wind direction to account for upwind terrain features, which is not measured across a basin scale, requiring a modeling approach (e.g., Liston and Sturm, 1998), thus it was not used in this study.

Canopy cover is a categorical measurement that was made in the field during manual snow surveys. If tree canopy was present above a sampling location, the canopy cover was assigned a value of one, and sampling locations with open canopy were assigned a value of zero. We expect canopy cover to show a negative correlation with SWE. Canopy density can influence how snow is distributed across space as it is directly related to the amount of snow that is intercepted in the tree canopy. Snow sublimation from snow intercepted within the forest canopy is a major component of the overall water balance (Pomeroy and Gray, 1995; Montesi et al., 2004).

Multiple linear regression was used to model 2 April 2011 and 31 March 2012 SWE based on its relation with the following independent physiographic variables: UTM Easting, UTM Northing, elevation, slope, northness, eastness, solar radiation, curvature, and canopy cover. A detailed description of the multiple linear regression methodology is provided above. Multiple linear regression models were developed using both operational and field snowpack measurements and also operational measurements only. At this scale of interest, operational data are commonly the only snowpack data available, thus it was useful to compare the results from operational data only to those results obtained from using operational data and additional field-based measurements. The following notation will be used in this study: model_{O+F} will refer to the multiple regression model using both operational and field snow measurements, and model_O will refer to the multiple regression model using only operational snow measurements. A total of four regression models were developed: model_{O+F11} (operational and field data from 2011), model_{O11} (operational data from 2011), model_{O+F12} (operational and field data from 2012), and model_{O12} (operational data from 2012).

4 Results

4.1 Snow density model

The pairwise relations between snow depth, snow density, and SWE from the historic snow course records are presented in Fig. 3. A strong correlation exists between snow depth and SWE, which is best fit as a power function (Fig. 3a). There is considerable scatter about the linear fit for snow density versus snow depth (Fig. 3b), which suggests that additional variables should be included to describe the variability of snow density. Snowpack relations shown here are similar to those found in previous studies (e.g., Jonas et al., 2009; Sturm et al., 2010).
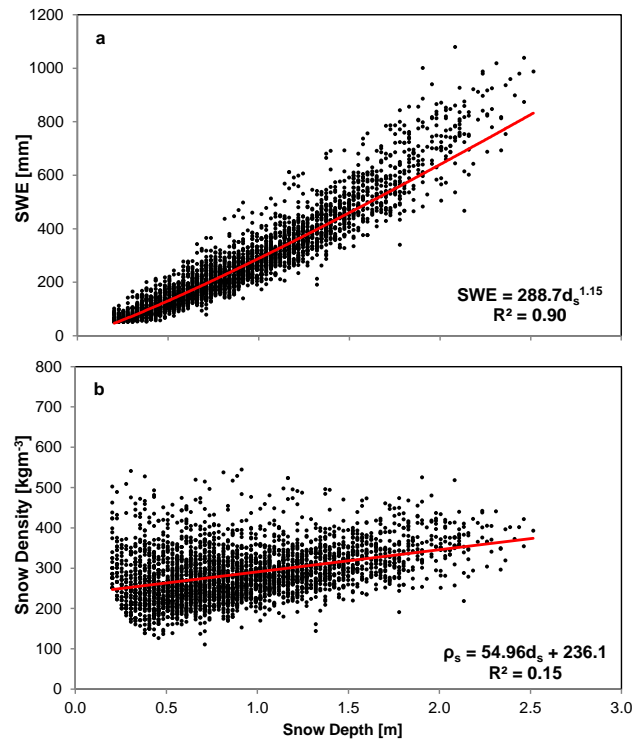

Fig. 3. Pairwise relations of SWE and snow density with snow depth from historic snow course measurements within the study area.

The mean snow density from the snow course data set is $287\,\text{kg}\,\text{m}^{-3}$ with a standard deviation of $64.8\,\text{kg}\,\text{m}^{-3}$. SWE and snow depth have a greater coefficient of variation (0.65, 0.50, respectively) compared to snow density (0.23). Snow density is most highly correlated with Julian day, and also shows a positive correlation with snow depth and elevation and negative correlation with UTM Easting (Table 1). The location-dependent correlation with snow density has been shown in previous studies (e.g., Mizukami and Percia, 2008), however, is often based on a larger domain and is representative of differences in climatology. The correlation of UTM Easting and snow density found from this basin scale data set may be representing the impact of the distance to a mountain barrier or storm track patterns on snow density patterns.

The final snow density model takes the following form:

$$\rho_s = 844 + 1.06\text{DOY} + 26.1\,d_s^{0.5}$$
$$+ 4.0 \times 10^{-2}z - 1.78 \times 10^{-3}\text{UTM}_e, \tag{1}$$

where ρ_s is snow density, DOY is Julian day, d_s is snow depth, z is elevation, and UTM_e is UTM Easting. A square root transformation of snow depth was made to satisfy model assumptions. All variables included were shown to have statistical significance ($p < 0.05$). The variance inflation factor (VIF) is less than 2.2 for each variable within the final model, suggesting that multicollinearity between independent variables is not observed. The residuals of the regression

Table 1. Historic snow course bivariate correlations between snow density, SWE, snow depth, Julian day, elevation, UTM Northing, and UTM Easting and snow density model calibration and validation performance statistics. Performance statistics for snow water equivalent based on using modeled snow density and observed snow depth to calculate SWE. Bolded values represent statistical significance (p value < 0.05).

	Snow density	SWE
Bivariate correlations		
Snow depth	**0.39**	**0.94**
Day of year	**0.62**	**0.33**
Elevation	**0.24**	**0.60**
UTM Northing	−0.03	**−0.15**
UTM Easting	**−0.35**	**−0.43**
Snow density Model performance		
R^2	0.51	0.94
RMSE	45.4 kg m^{-3}	44.2 mm
Snow density model Validation (RMSE)		
Field measurements ($n = 84$)	44.7 kg m^{-3}	70.3 mm
SNOTEL ($n = 121$)	62.7 kg m^{-3}	56.7 mm

model are normally distributed and do not violate the underlying assumptions of the regression (normality, linearity, homoscedasticity).

The calibrated model underestimated more dense snowpacks and overestimated less dense snowpacks, while calculated SWE showed generally unbiased residuals that tended to slightly increase with increasing observed SWE (Fig. 4). Performance statistics calculated from the residuals of calibration with the original data set showed that predicted snow density explained 51 % of the total variance in the data with a RMSE of 45.4 kg m^{-3}, yet, calculated SWE was able to explain 94 % of the variance in the data and had a RMSE of 44.2 mm (Table 1).

Various methods of model evaluation were performed to test the utility of the regression model that all showed similar trends (Fig. 4) and comparable error estimates (Table 1) to model calibration. As expected, a minor increase in error estimation was observed for model validation with independent data, yet the minimal increase in error shows that the regression model should be transferable to independent data within the bounds of the original data set. Thus, we used the snow density model to calculate SWE for WY 2011 and WY 2012 field-based snow depth measurements.

4.2 Basin scale SWE variability

A total of 51 and 127 snowpack measurements (both operational and field-based) were analyzed from the 2 April 2011 (WY 2011) and 31 March 2012 (WY 2012) snow surveys, respectively (Fig. 1). The mean SWE and snow depth from WY 2011 were greater than WY 2012, yet the mean snow density and standard deviation of snow density was shown to be consistent among both years (Table 2). The WY 2011 was the maximum snow year on record within the study area, while WY 2012 was one of the lowest snow years on record (Fig. 2); thus WY 2011 snowpack measurements were shown to have a higher mean SWE and snow depth, but also had a greater range of variability than that of WY 2012 (Table 2). From the average SWE among SNOTEL stations within the study area, the 1 April snow survey occurred before peak SWE in 2011, however, it occurred slightly after peak SWE yet before substantial melt had occurred in 2012. Analysis of the 1 April snowpack from these two water years allows for the comparison between the two extreme snow years (maximum and minimum) as well as between two different stages of the niveograph (before and just after peak SWE).

In order to evaluate whether the physiographic variables that were sampled in this study are representative of their basin scale distributions, we have made comparisons between the values associated with the sampling locations compared to the values across the study area. Terrain variables derived within GIS at each of the snowpack measurement locations have similar averages when compared to the 50 % Snow Cover Index (SCI) (Richer et al., 2013) (Fig. 1), for both 2011 and 2012. Histograms of relative frequency (Fig. 5) show that the distribution of terrain variables sampled in 2011 and 2012 is similar to the 50 % SCI area distribution of these variables, suggesting that the snowpack measurement locations sampled during WY 2011 and WY 2012 are representative of the variability of physiography among the entire study area. The range of values of terrain variables observed at operational stations tended to be smaller than the field-based station ranges (Fig. 5), which also suggests the combination of operational and field-based measurements are more representative of the basin than the operational measurements alone. A formal Kolmogorov–Smirnov test (K-S test) for equality of distributions between a random sample ($n = 244$) of the continuous terrain variables within the 50 % SCI area of the basin versus the variables associated with each WY's sampling locations was completed. The K-S test shows that during both years the difference between the two samples for curvature and eastness is not significant enough (95 % significant level) to say they have a different distribution. However, a significant difference between the distributions of elevation, slope, northness, and solar radiation was observed for both years. The difference in elevation is obvious since field data are located more at higher elevations than the entire domain (Fig. 5a), and the operational data tend to be located in a small elevation zone (Fassnacht et al., 2012). Northness is highly correlated to solar radiation, and both are related to slope so the significance difference for each of these variables is partly based on their correlation. For avalanche safety purposes, manual measurements
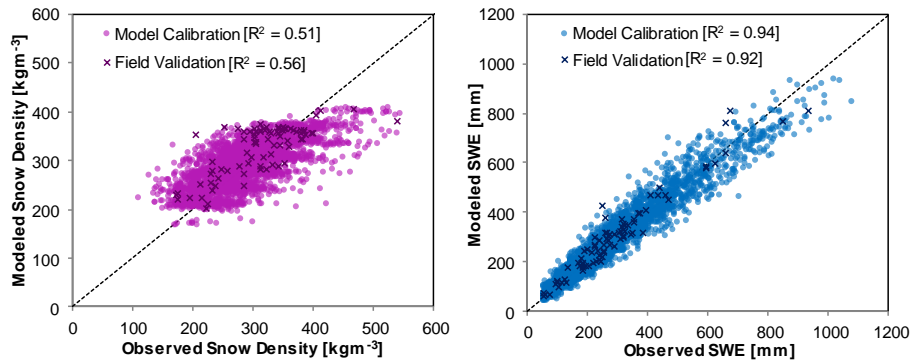
Fig. 4. Snow density model versus observed snow density and SWE calibration with historic snow course data and validation with independent field data. Modeled SWE is derived from modeled snow density and observed snow depth.

Table 2. Summary statistics (μ = mean, σ = standard deviation) for snowpack properties from WY 2011 and WY 2012 snow surveys. Statistics calculated separately for manual and operational measurements as well as manual measurements in which SWE was estimated from the snow density model.

	n	SWE (mm)		ρ_s (kg m^{-3})		d_s (m)	
		μ	σ	μ	σ	μ	σ
WY 2011							
Field measurements	28	356	259	307	37.0	1.10	0.68
Field SWE measurements	11	357	242	309	46.7	1.09	0.60
Estimated SWE	17	356	276	305	30.7	1.10	0.74
SNOTEL measurements	10	577	220	342	38.2	1.66	0.55
Snow course measurements	13	410	239	304	24.5	1.31	0.66
Entire data set	51	413	256	313	36.9	1.26	0.68
WY 2012							
Field measurements	104	228	106	313	23.9	0.72	0.30
Field SWE measurements	12	264	69	318	44.7	0.85	0.26
Estimated SWE	92	224	109	312	20.0	0.70	0.31
SNOTEL measurements	10	241	113	324	69.9	0.72	0.33
Snow course measurements	13	152	105	285	50.4	0.52	0.32
Entire data set	127	221	108	311	33.8	0.70	0.31

are usually on slopes less than 35°, so steeper slopes can be underrepresented.

Snowpack variables were shown to have a strong correlation with each other, with SWE and snow depth showing the strongest relation (consistent with the historic snow course data set), while also showing to be highly correlated with elevation (Table 3). Bivariate relations showed that SWE increased with increasing elevation, with the steepness of this trend being greater in WY 2011 than 2012. The strength of the correlation between SWE and elevation for WY 2011 ($r = 0.75$) and WY 2012 ($r = 0.68$) suggests that elevation is the most important physiographic variable for driving the distribution of SWE across the study domain, which is consistent with previous findings from studies evaluating SWE at the basin scale (e.g., Fassnacht et al., 2003; Jost et al., 2007; Harshburger et al., 2010). As UTM Northing increases, SWE

decreases in WY 2011, suggesting northern regions of the study area receive less snow than southern regions (as suggested by J. Meiman, personal communication, 2010), yet this trend was not apparent in the low snow year of 2012. Our sample size is only two years, therefore additional basin scale data are needed to evaluate snow distributions in relation to UTM Northing, however, historic trends observed from the SNOTEL data suggest that lower snow amounts in the northern parts of the study area (similar to WY2011) may be more common (Fig. 2). A greater accumulation of snow in southern regions of the study area could be related to an upwind elevation gradient, with high peaks of Rocky Mountain National Park located in the southern portion of the study area, or due to the possibility of a dominant storm track that preferentially precipitates in southern regions before moving northward. SWE also decreased with increasing
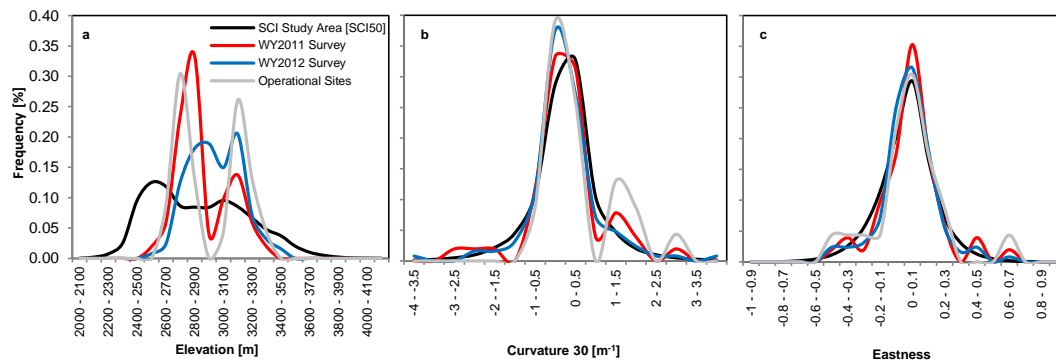
Fig. 5. Histograms of terrain variables across the SCI 50 study area compared to variables associated with snow measurement locations.

UTM Easting, which corresponds to both the effect of orographic precipitation within the study area (the continental divide is located on the western border of the study area), and also lower elevation regions receiving less snow than higher-elevation regions. The other variables that are known to influence snow accumulation (e.g., forest cover and solar radiation) did not exhibit strong bivariate correlations with SWE, thus partial correlations were calculated to test these variables once the trends of elevation and UTM coordinates had been removed. The partial correlation is defined as the correlation between two variables, while the effect of a set of controlling variables is removed (through linear regression). Partial correlations between SWE and terrain/canopy variables (with the correlation effect of elevation, UTM Easting, and UTM Northing removed) shows that curvature and slope become more important variables when the other trends are removed (Table 4).

Multiple linear regression was used to model SWE for 2 April 2011 and 31 March 2012 with the operational and field-based snowpack data set (model$_{O+F}$) and the operational snowpack data set only (model$_O$) (Fig. 6). The final independent variables used within each model, beta coefficient values, and a summary of model performance statistics is provided in Table 5 and Fig. 6. To satisfy the assumptions of the regression model and improve overall model performance, a square root transformation was made to SWE (dependent variable) and slope (independent variable) for model$_{O+F11}$, which explains 88 % of the total variance with an RMSE of 85.6 mm (all RMSE values were calculated after transformed values have been converted back). Model$_{O+F12}$ (no data transformations) explained 56 % of the total variance and showed an RMSE of 71.5 mm. The operational models were evaluated against observed values from the entire operational and field data set. The WY 2011 operational model (model$_{O11}$) explains 84 % of the total variance of the data with an RMSE of 110.1 mm and includes a square root transformation of SWE. Lastly, model$_{O12}$ explains 51 % of the total variance with a RMSE of 75.6 mm. The VIF is less than 1.4 for each variable within all four of the multiple regression models, suggesting that multicollinearity between independent variables is not observed. Also, the residuals of each regression model do not violate the underlying assumptions of the regression (normality, linearity, homoscedasticity).

A comparison of the standardized error estimation between WY 2011 and WY 2012 models shows that the model$_{O+F11}$ has a lower standardized typical magnitude of error (standardized RMSE) than model$_{O+F12}$, and describes more of the variance in the data (R^2) (Table 5). Similarly, model$_{O11}$ has a lower standardized RMSE and greater R^2 value than model$_{O12}$, but the difference between these two models is less (Table 5). The difference among these performance statistics can partially be explained by the nature of each snow year (WY 2011 was the maximum snow year and WY 2012 was amongst the lowest) and sampling scheme. WY 2011 showed much more variation in snow amounts than WY 2012, which could explain the difference in the RMSE. Additionally, the greater number of measurement locations ($n = 127$) in WY 2012 compared to WY 2011 ($n = 51$) could further explain the difference in R^2 between model$_{O+F11}$ and model$_{O+F12}$. Given this difference in field-based sampling locations, a reduced model$_{O+F}$ for WY 2012 was developed, including only WY 2012 field-based measurement locations that were co-located with WY 2011 measurement locations ($n = 42$). The reduced model included UTM Northing, elevation, and curvature 30 as independent variables and explained 70 % of the total variance with a standardized RMSE of 30 % (Fig. 6). The reduced model shows more favorable results than the full model (model$_{O+F12}$), suggesting that fewer data points may be the reason for the stronger performance of the WY 2011 models. However, the reduced model also explained less of the variance in the data than model$_{O+F11}$, which suggests that the superior performance of the 2011 models could be due to the greater range of observed variability in the data.

5 Discussion

The snow density model developed across the study area performed relatively well in modeling SWE from independent

Table 3. Bivariate correlations between SWE, snow density, snow depth, and terrain and canopy variables for the water year 2011 and 2012 snow surveys. Bolded values represent statistical significance (p value < 0.05).

	WY 2011			WY 2012		
	SWE	ρ_s	d_s	SWE	ρ_s	d_s
SWE (mm)	–	–	–	–	–	–
Snow density (kg m^{-3})	**0.81**	–	–	**0.52**	–	–
Snow depth (m)	**0.99**	**0.75**	–	**0.98**	**0.40**	–
Elevation (m)	**0.75**	**0.46**	**0.77**	**0.68**	**0.41**	**0.67**
UTM Easting (m)	**−0.69**	**−0.71**	**−0.66**	**−0.38**	**−0.51**	**−0.33**
UTM Northing (m)	**−0.55**	−0.36	**−0.56**	−0.12	−0.02	−0.10
Eastness	−0.13	**−0.28**	−0.11	0.10	−0.09	0.13
Northness	−0.01	−0.08	0.00	0.06	−0.13	0.08
Canopy cover	−0.20	−0.16	−0.21	**−0.22**	−0.01	**−0.22**
Slope (°)	−0.03	−0.05	−0.01	0.11	0.05	0.13
Curvature 30 (m^{-1})	0.08	0.13	0.08	−0.08	−0.11	−0.04
Curvature 100 (m^{-1})	−0.04	−0.02	−0.02	−0.08	−0.08	−0.06
Solar radiation (W m^{-2})	0.26	0.20	0.25	0.07	**0.22**	0.04

Table 4. Partial correlations between SWE and terrain/canopy variables with the effect of elevation (z), UTM Easting (x), and UTM Northing (y) removed. Bolded values represent statistical significance (p value < 0.05).

	WY 2011		WY 2012	
	z	z, x, y	z	z, x, y
UTM Easting (m)	**−0.74**	–	−0.16	–
UTM Northing (m)	**−0.38**	–	**0.16**	–
Eastness	−0.07	0.23	0.08	0.10
Northness	0.06	0.18	0.12	0.16
Canopy cover	−0.14	0.06	−0.15	−0.17
Slope (°)	−0.22	**−0.28**	**−0.08**	**−0.06**
Curvature 30 (m^{-1})	−0.07	**−0.41**	**−0.32**	**−0.31**
Curvature 100 (m^{-1})	−0.25	**−0.31**	**−0.36**	**−0.35**
Solar radiation (W m^{-2})	0.02	−0.10	−0.06	−0.13

snow depth measurements. Predicted SWE RMSE ranged from 44 mm (calibration data) to 70 mm (independent field validation data). Eighty percent of all residual values ($n = 2613$) fell within ± 50 mm, and the variance of the model residuals was on average within 12.8 % of the observed values for the calibration data set. Within site variability of SWE has been conservatively estimated to be 15 to 25 % (Jonas et al., 2009), which suggests that the error observed from the model is within the natural range of SWE variability at a site (Fassnacht et al., 2008). The small range of error suggests that estimating SWE from snow depth measurements through a snow density model works due to the conservative nature of snow density; 52 % of snow density data values ranged from 250 to 350 kg m^{-3}.

Using historical operational measurements for development of a basin scale snow density model has implications for future field-based basin scale sampling campaigns, suggesting a sampling scheme dominated by snow depth measurements may be successful for evaluating basin scale SWE variability. The strength and utility of the model developed here is its ability to estimate SWE from the most easily measured variable, snow depth. Across basin scales, efforts are being made to estimate snow depth using both airborne lidar and satellite-based lidar data, such as ICESat (Jasinski et al., 2012). Snow density models will be especially useful for these applications. The utility of a snow density model is also very valuable for field-based snow surveys at the basin scale, in which many snowpack measurements are required, and the assumption of a constant snow density across the study area is not valid (Lopéz-Moreno et al., 2013).

The snow density model is simple to develop and implement and is an effective tool for obtaining estimates of SWE from snow depth measurements across basin scale domains. The model is, however, constricted to its spatial domain, range of physiographic inputs, as well as temporal coverage, thus it may not be applicable to areas outside of the study area for elevations that are lower than 2408 m or higher than 3261 m, or for snow depths shallower than 0.20 m or deeper than 2.52 m.

Given that our snow density model was calibrated specifically for the Cache la Poudre Basin, it is useful to compare its performance to similar snow density models that have been developed from historic data for different domains. Jonas et al. (2009) developed a set of regression equations to model snow density using snow depth, day of year, elevation, and region for the Swiss Alps, while Sturm et al. (2010) employed a statistical method based on Bayesian analysis for the United States, Canada, and Switzerland using snow depth, day of year, and climate class. These previous studies and our research show that snow density is a conservative variable that varies spatially much less than snow depth and SWE, however the previous studies used spatial domains

Table 5. Beta coefficients (standardized coefficients) and performance statistics for each multiple regression model with dependent variable SWE (mm). Each coefficient included in the models was statistically significant (p value < 0.05). Model performance metrics are evaluated against the entire data set (both operational and field) for each year. RMSE and MAE statistics are reported as standardized values (value of the statistic divided by the mean of the observations).

	model$_{O+F11}$	model$_{O11}$	model$_{O+F12}$	model$_{O12}$	Reduced model$_{O+F12}$
n values	51	23	127	23	42
Beta coefficients					
Elevation (m)	0.52	0.76	0.77	0.98	0.89
UTM Easting (m)	−0.51	−0.45	–	–	–
UTM Northing (m)	−0.23	–	0.13	0.43	0.21
Canopy cover	–	–	−0.14	–	–
Slope$^{0.5}$ (°)	−0.12	–	–	–	–
Curvature 30 (m^{-1})	−0.16	−0.21	–	–	−0.36
Curvature 100 (m^{-1})	–	–	−0.28	−0.34	–
Model performance					
R^2	0.88	0.84	0.56	0.51	0.70
RMSE (%)	21	27	32	34	30
MAE (%)	16	22	25	26	26

that are orders of magnitude larger than what has been presented here, with the current data being at a finer resolution. We have applied the snow density alpine model developed by Sturm et al. (2010) to our data set and directly compared the results to those of our snow density model, given their model was developed for global applications and data from the western US were used within model development. We did not, however, test the model developed by Jonas et al. (2009), as it was developed specifically for Switzerland and requires regional and elevational parameters that are specific to this area, and was not developed for use in other areas. The Sturm et al. (2010) alpine model performed well when applied to the data set from this study, showing a snow density RMSE of $58.1\,\mathrm{kg\,m^{-3}}$ and RMSE of $53.4\,\mathrm{mm}$ when used to calculate SWE. Also, the variance described in the SWE data set from this study by the Sturm et al. (2010) model showed a similarly strong performance ($R^2 = 0.91$) as our model. However, the model developed in this study outperformed the Sturm et al. (2010) model, showing an improvement in RMSE for snow density and SWE by 22 % and 17 %, respectively. Also, our model showed an improvement of field validation RMSE by 9 % for snow density and 7 % for SWE. This shows that calibrating a snow density model to a specific basin of interest can improve estimates of SWE from snow depth from models developed from larger domains and should be considered for future basin scale assessments of SWE.

Despite WY 2011 being a maximum snow year and WY 2012 being a minimum year, the variables driving each SWE regression were similar and included elevation, location within the basin (UTM Easting and/or UTM Northing),

and curvature. The inclusion of elevation and geographic location within each regression as well as the strong bivariate correlations of these variables with SWE indicates that they may be representing consistent drivers of the spatial variability of SWE at the basin scale, such as how orographic precipitation and storm track patterns play a strong role in basin scale SWE distribution. Additionally, the inclusion of terrain curvature within each model suggests that wind redistribution of snow is also important at this scale. However, model results of other variables suggest limitations due to the representivity of their basin scale distributions. The slopes that were sampled in this study were not generally steep (for safety considerations) and were below the common critical angle of repose for snow avalanches (McClung and Schaerer, 2006), however, this variable was shown to have a significant negative partial correlation with SWE distribution during both years. Given the slopes sampled in this study, we suggest the significance of the slope variable may not actually represent a driver of basin scale variable, but rather a statistical artifact. Also, the importance of solar radiation on the distribution of the snowpack has been highlighted by previous studies conducted in both alpine (e.g., Erikson et al., 2005) and forested areas (e.g., Veatch et al., 2009), however solar radiation was not shown to be a significant explanatory variable of basin scale snow variability in this study. Solar radiation is likely an important control on basin scale snow distribution, therefore the lack of significance of this variable is because it was neither adequately sampled nor modeled. The sampled locations in this study were not representative of the solar radiation variability across the basin, as shown by the K-S test. Also, modeled clear-sky solar radiation does not
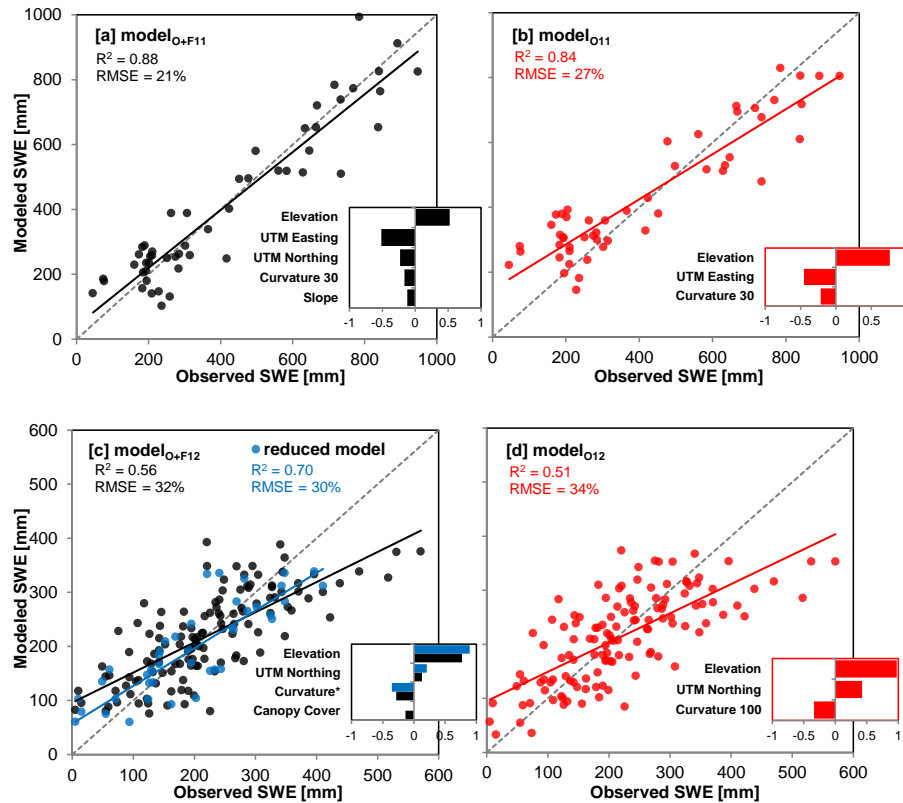
Fig. 6. Scatterplots showing observed versus modeled SWE from model$_{O+F}$ (shown in black) and model$_O$ (shown in red) for both WY 2011 and 2012. The observed values used to evaluate each model include the combined operational and field-based data set. The reduced model$_{O+F12}$ includes only field-based measurement locations also sampled during WY 2011 (shown in blue). The callout bar graphs show the relative influence of each model coefficient (beta coefficients). Curvature* represents curvature 100 for model$_{O+F12}$ and curvature 30 for the reduced model.

take into the account shading from tree canopy, therefore it is not representative of solar radiation across the basin scale. Additionally, although the canopy cover variable did show the negative correlation with SWE as expected, this correlation was relatively weak, thus the categorical canopy cover variable we use here is likely not adequate. There is a need for a finer resolution canopy data set for basin scale analyses, as the 30 m-resolution National Land Cover Database (NLCD 2001) canopy density data are not adequate; this data set often shows SNOTEL stations as having high canopy density values despite their location within small forest openings. Future basin scale snow studies should focus on incorporating a more accurate representation of the influence of forest canopy and solar radiation on snowpack variability (Musselman et al., 2013). Given that studies (e.g., Fassnacht et al., 2012) have shown the spatial variability of snow accumulation to be described by different physiographic variables from year to year, additional years of data collection at the basin scale are needed for a more complete evaluation of the drivers of SWE distribution.

Comparison of the error between model$_{O+F}$ and model$_O$ for WY 2011 and WY 2012 shows that model$_{O+F}$ has

superior performance statistics for both years (Table 5). Model$_{O+F}$ showed a 22 % and 5 % improvement in RMSE from model$_O$ in 2011 and 2012, respectively. However, model$_{O11}$ and model$_{O12}$ showed a fairly strong performance with similar predictor variables as the operational plus field models. The operational regression models may not be representing the study area, as SNOTEL measurements have been shown to represent point locations rather than surrounding areas (Molotch and Bales, 2005) often having more snow (Daly et al., 2000), and tend to be located in areas with similar physiographic features (flat and open canopy areas located near tree line).

The spatial data set of field-based snowpack measurements in this study is at a scale similar to remote sensing observations and modeling applications; these data and the approaches of empirical modeling (e.g., multiple linear regression) for characterizing the distribution of SWE at the basin scale can be used in those contexts for validation. For instance, the observed patterns of SWE variability within this study, showing to be largely driven by elevation and geographic location, could be compared to the patterns of variability observed within a physically based snow evolution
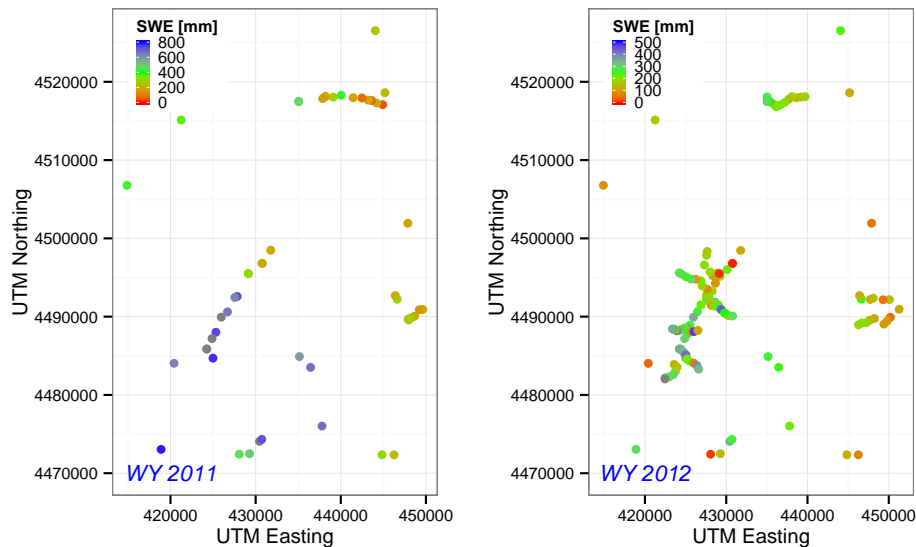
Fig. 7. SWE plotted against UTM Northing and UTM Easting for both WY 2011 and WY2012 snow surveys.

model. The comparisons of the statistical relation of the snowpack with terrain-based variables and physically based snow evolution modeling can provide insight for basin scale SWE distribution estimations.

There are limitations to this study that must be acknowledged. The representivity of snow measurements of their surroundings is an important issue often raised in snow hydrology studies (e.g., Molotch and Bales, 2005). Although our field-based measurements attempted to account for the fine-scale variability by taking 11 measurement points at each sampling location, it is possible these sampling locations could have fallen on the edge of a 30 m-resolution GIS pixel and not accurately sampled associated terrain variables. The SNOTEL station snow pillows have been shown to not represent their surroundings, which could have caused further inaccuracies of the DEM-derived variables at each of these sites. The use of multiple linear regression to model non-linear processes for the SWE models developed within this study is another important limitation. Limitations in this approach have been presented in previous studies (Elder et al., 1995), however, we do believe that multiple linear regression was appropriate given the goals of our study. We would have ideally used binary regression trees (e.g., Elder et al., 1998) to develop the SWE models, but these decision tree models require larger datasets than available in this study to provide meaningful results. Given the main goal of the SWE models was used as a tool to evaluate the importance of individual variables rather than used strictly within a predictive framework, the multiple linear regression models provide simplicity of the interpretation of model coefficients. Finally, our field sampling strategy (non-uniform, non-random spacing, and clustered pattern), which is a different spacing than operational data, may have influenced regression results. Given the extent of the study area evaluated (1493 km^2), it was nec-

essary to employ this transect-based strategy because of the formidable challenge of accessing these areas throughout the basin on skis. Each sampling transect with 500 m spacing of sampling locations were generally around four kilometers in length and located along an elevational gradient with varying terrain, providing a range of snow conditions to be sampled (Fig. 1). Further evaluation of each of the individual sampling clusters (Colorado State University Pingree Park Campus, Cameron Pass, and Deadman Hill) showed that elevation and location have the strongest correlation with SWE, suggesting the 500 m spacing of the field-based sampling locations is likely large enough to represent our scale of interest. A plot of UTM Easting and UTM Northing versus SWE (Fig. 7) shows clear regional trends of the distribution of SWE across the study area. The importance of the UTM coordinates in describing the SWE distribution is likely not being affected by the sampling clusters, as these same trends were observed from the operational data (model$_O$). Future snow field campaigns at the basin scale should take strong consideration of the best sampling strategy suited for the challenges of covering the basin scale.

6 Conclusions

We have used a combination of operational and field-based snow measurements to evaluate snowpack properties across the basin scale. This research was motivated by the need for additional ground-truth snowpack observations at a scale that coincides with that of remote sensing observations and is especially pertinent to water resources forecasting.

A method for modeling snow density across the Cache la Poudre Basin from historical snow course measurements was employed for estimating SWE from snow depth. The

independent variables of snow depth, day of year, elevation, and UTM Easting were used in a multiple linear regression model to estimate snow density. Statistics showed strong performance of SWE calculated from snow depth observations using the snow density model, and model validation suggests the model is transferable to independent data within the bounds of the original data set. The methods here provide a pathway for estimating SWE from snow depth measurements, which is especially useful when evaluating snowpack properties at the basin scale, where time-consuming field-based measurements of SWE are often not feasible.

The spatial variability of SWE within the Cache la Poudre Basin was analyzed using operational and field-based snowpack measurements from WY 2011 and WY 2012. Bivariate and partial correlations of SWE with terrain and canopy variables as well as multiple linear regression models show that elevation, UTM Easting, UTM Northing, and curvature are most highly correlated with SWE during both years, and thus likely are explanatory variables describing processes that drive spatial variability at this scale (e.g., orographic precipitation, synoptic weather patterns, and wind redistribution of snow). Solar radiation is also likely one of the main drivers of basin scale snow variability, however this variable was neither adequately sampled nor modeled in this study, suggesting its lack of significance may have been a misrepresentative statistical finding.

The continuity of field-based snowpack measurements, as provided within this study, is essential given the assumption of non-stationarity from hydroclimatic change (Milly et al., 2008) and indications of more extreme conditions (IPCC, 2007). This examination of two very different snow years may represent the bounds of extremes and possibly the limitations due to non-stationarity. Continued field measurements of the snowpack will aid advancement of remote sensing and modeling applications, but more importantly continue to provide ground-truth observations for evaluating the complexities and uncertainties of the changing earth system.

Edited by: D. Hall

References

Akaike, H.: A new look at the statistical model identification, IEEE T. Automat. Contr., 19, 716–723, 1974.

Anderton, S. P., White, S. M, and Alvera, B.: Evaluation of spatial variability in snow water equivalent for a high mountain catchment, Hydrol. Process., 18, 435–453, 2004.

Bales, R. C., Molotch, N. P., Painter, T. H., Dettinger, M. D., Rice R., and Dozier, J.: Mountain hydrology of the western United States, Water Resour. Res., 42, W08432, doi:10.1029/2005WR004387, 2006.

Balk, B. and Elder, K.: Combining binary decision tree and geostatistical methods to estimate snow distribution in a mountain watershed, Water Resour. Res., 36, 13–26, 2000.

Barry, R. G.: Mountain Weather and Climate, 3rd Edn., Cambridge University Press, Cambridge, 2008.

Berk, K. N.: Comparing Subset Regression Procedures, Technometrics, 20, 1–6, 1978.

Blöschl, G.: Scaling issues in snow hydrology, Hydrol. Process., 13, 2149–2175, 1999.

Blöschl, G., Kirnbauer, R., and Gutknecht D.: Distributed Snowmelt Simulations in an Alpine Catchment 1. Model Evaluation on the Basis of Snow Cover Patterns, Water Resour. Res., 27, 3171–3179, 1991.

Clow, D. W.: Changes in the Timing of Snowmelt and Streamflow in Colorado: A Response to Recent Warming, J. Climate, 23, 2293–2306, 2010.

Daly, S. F., Davis, R., Ochs, E., and Pangburn, T.: An approach to spatially distributed snow modeling of the Sacramento and San Joaquin basins, California, Hydrol. Process., 14, 3257–3271, 2000.

Dingman, S. L.: Elevation: A major influence on the hydrology of New Hampshire and Vermont, USA, Hydrol. Sci. Bull., 26, 399–413, 1981.

Doesken, N. J. and Judson, A.: The Snow Booklet: A Guide to the Science, Climatology, and Measurement of Snow in the United States, Dep. of Atmos. Sci., Colorado State Univ., Fort Collins, CO, 1996.

Dressler, K., Fassnacht, S. R., and Bales, R. C.: A Comparison of Snow Telemetry and Snow Course Measurements in the Colorado River Basin, J. Hydrometeorol., 7, 705–712, 2006.

Elder, K., Dozier, J., and Michaelson, J.: Snow accumulation and distribution in an Alpine watershed, Water Resour. Res., 27, 1541–1552, 1991.

Elder, K., Michaelsen, J., and Dozer, J.: Small basin modelling of snow water equivalence using binary regression tree methods, Proc. Symp. on Biogeochemistry of Seasonally Snow-Covered Catchments, Boulder, CO, IAHS-AIHS and IUGG XX General Assembly, IAHS Publication 228, 129–139, 1995.

Elder, K., Rosenthal, W., and Davis, R. E.: Estimating the spatial distribution of snow water equivalence in a montane watershed, Hydrol. Process., 12, 1793–1808, 1998.

Erickson, T. A., Williams, M. W., and Winstral, A.: Persistence of topographic controls on the spatial distribution of snow in rugged mountain terrain, Colorado, United States, Water Resour. Res., 41, W04014, doi:10.1029/2003WR002973, 2005.

ESRI: ArcGIS Desktop: Release 10. Redlands, CA: Environmental Systems Research Institute, 2011.

Fassnacht, S. R., Dressler, K. A., and Bales, R. C.: Physiographic parameters as indicators of snowpack state for the Colorado

River Basin, Proceedings of 58th Eastern Snow Conference, Ottawa, Ontario, Canada, May 2001.

Fassnacht, S. R., Dressler, K. A., and Bales, R. C.: Snow water equivalent interpolation for the Colorado River Basin from snow telemetry (SNOTEL) data, Water Resour. Res., 39, 1208–1218, 2003.

Fassnacht, S. R., Skordahl, M. E., and Derry, J. E.: Variability at Colorado Operational Snow Measurement Sites, Snowcourse Stations at Collocated Snow Telemetry Stations, Proceedings of 65th Eastern Snow Conference, Fairlee, Vermont, USA, May 2008.

Fassnacht, S. R., Heun, C. M., López-Moreno, J. I., and Latron, J. B. P.: Variability of Snow Density Measurements in the Rio Esera Valley, Pyrenees Mountains, Spain, Cuadernos de Investigación Geográfica J. Geogr. Res., 36, 59–72, 2010.

Fassnacht, S. R., Dressler, K. A., Hulstrand, D. M., Bales, R. C., and Patterson, G.: Temporal Inconsistencies in Coarse-Scale Snow Water Equivalent Patterns: Colorado River Basin Snow Telemetry-Topography Regressions, Pirineos, 167, 167–186, 2012.

Harshburger, B. J., Humes, K. S., Walden, V. P., Blandford, T. R., Moore, B. C., and Dezzani, R. J.: Spatial interpolation of snow water equivalency using surface observations and remotely sensed images of snow-covered area, Hydrol. Process., 24, 1285–1295, 2010.

Intergovernmental Panel on Climate Change (IPCC): Climate Change 2007: The Physical Science Basis: Contribution of Working Group I to the Fourth Assessment Report of the IPCC, edited by: Solomon, S., Qin, D., Manning, M., Chen, Z., Marquis, M., Averyt, K. B., Tignor, M., and Miller, H. L., Cambridge Univ. Press, Cambridge, UK, 2007.

Jasinski, M., Stoll, J., Carabajal, C., and Harding, D.: Feasibility of Estimating Snow Depth in Complex Terrain Using Satellite Lidar Altimetry, Eastern Snow Conference, Claryville, NY, 5–12 June 2012, 2012.

Jepsen, S. M., Moltch, N. P., Williams, M. W., Rittger, K. E., and Sickman, J. O.: Interannual variability of snowmelt in the Sierra Nevada and Rocky Mountains, United States: Examples from two alpine watersheds, Water Resour. Res., 48, W02529, doi:10.1029/2011WR011006, 2012.

Jonas, T., Marty, C., and Magnusson, J.: Estimating the snow water equivalent from snow depth measurements in the Swiss Alps, J. Hydrol., 378, 161–167, 2009.

Jost, G., Weiler, M., Gluns, D. R., and Alila, Y.: The influence of forest and topography on snow accumulation and melt at the watershed-scale, J. Hydrol., 347, 101–115, 2007.

Kerr, T., Clark, M., Hendrikx, J., and Anderson, B.: Snow distribution in a steep mid-latitude alpine catchment, Adv. Water Resour., 55, 17–24, 2013.

Kimerling, A. J., Buckley, A. R., Muehrcke, P. C., and Muehrcke, J. E.: Map Use: Reading Analysis Interpretation, Seventh Edition, ESRI Press Academic, Redlands, California, 2011.

Kutner, M. H., Nachtsheim, C. J., Neter, J., and Li, W.: Applied Linear Statistical Models, Fifth Edition. McGraw-Hill/Irwin, New York, NY, 2005.

Lapen, D. R. and Martz, L. W.: An investigation of the spatial association between snow depth and topography in a prairie agricultural landscape using digital terrain analysis, J. Hydrol., 184, 277–298, 1996.

Liston, G. E. and Sturm, M.: A snow-transport model for complex terrain, J. Glaciol., 44, 498–516, 1998.

Logan, L. A.: Basin-wide water equivalent estimation from snowpack depth measurements, IAHS-AISH P., 107, 864–884, 1973.

López-Moreno, J. I. and Nogués-Bravo, D.: Interpolating local snow depth data: an evaluation of methods, Hydrol. Process., 20, 2217–2231, 2006.

López-Moreno, J. I., Fassnacht, S. R., Beguería, S., and Latron, J. B. P.: Variability of snow depth at the plot scale: implications for mean depth estimation and sampling strategies, The Cryosphere, 5, 617–629, doi:10.5194/tc-5-617-2011, 2011.

López-Moreno, J. I., Fassnacht, S. R., Heath, J. T., Musselman, K. N., Revuelto, J., Latron, J., Morán-Tejeda, E., and Jonas, T.: Small scale spatial variability of snow density and depth over complex alpine terrain: Implications for estimating snow water equivalent, Adv. Water Resour., 55, 40–52, 2013.

Mallows, C. L.: Some Comments on C_p, Technometrics, 15, 661–675, 1973.

McClung, D. and Schaerer, P.: The Avalanche Handbook, Third Edition, The Mountaineers Books, Seattle, WA, 2006.

Milly P. C. D., Betancourt, J., Falkenmark, M., Hirsch, R. M., Zbigniew, W. K., Lettenmaier., D. P., and Stouffer, R. J.: Stationarity Is Dead: Whither Water Management?, Science, 319, 573–574, 2008.

Mizukami, N. and Perica, S.: Spatiotemporal characteristics of snowpack density in the mountainous regions of the Western United States, J. Hydrometeorol., 9, 1416–1426, 2008.

Molotch, N. P. and Bales, R. C.: Scaling snow observations from the point to the grid element: Implications for observation network design, Water Resour. Res., 41, W11421, doi:10.1029/2005WR004229, 2005.

Molotch, N. P., Colee, M. T., Bales, R. C., and Dozier, J.: Estimating the spatial distribution of snow water equivalent in an alpine basin using binary regression tree models: The impact of digital elevation data and independent variable selection, Hydrol. Process., 19, 1459–1479, 2005.

Montesi, J., Elder, K., Schmidt, R. A., and Davis, R. E.: Sublimation of Intercepted Snow within a Subalpine Forest Canopy at Two Elevations, J. Hydrometeorol., 5, 763–773, 2004.

Musselman, K. N., Margulis, S. A., and Molotch, N. P.: Estimation of solar direct beam transmittance of conifer canopies from airborne LiDAR, Remote Sens. Environ., 136, 402–415, 2013.

Pomeroy, J. W. and Gray, D. M.: Snow Accumulation, Relocation and Management. National Hydrology Research Institute Science Report No. 7, 1995.

R Development Core Team: R: A language and environment for statistical computing. R Foundation for Statistical Computing, Vievva, Austria, ISBN 3-900051-07-0, http://www.R-project.org/, 2012.

Richer, E. E., Kampf, S. K., Fassnacht, S. R., and Moore, C. C.: Spatiotemporal index for analyzing controls on snow climatology: Application in the Colorado Front Range, Phys. Geogr., 34, 85–107, doi:10.1080/02723646.2013.787578, 2013.

Stewart, I. T.: Changes in snowpack and snowmelt runoff for key mountain regions, Hydrol. Process., 23, 78–94, 2009.

Sturm, M., Taras, B., Liston, G. E., Derksen, C., Jonas, T., and Lea, J.: Estimating Snow Water Equivalent Using Snow Depth Data and Climate Classes, J. Hydrometeorol., 11, 1380–1394, 2010.

Viviroli, D., Weingartner, R., and Messerli, B.: Assessing the Hydrological Significance of the World's Mountains, Mt. Res. Dev., 23, 32–40, 2003.

Viviroli, D., Archer, D. R., Buytaert, W., Fowler, H. J., Greenwood, G. B., Hamlet, A. F., Huang, Y., Koboltschnig, G., Litaor, M. I., López-Moreno, J. I., Lorentz, S., Schädler, B., Schreier, H., Schwaiger, K., Vuille, M., and Woods, R.: Climate change and mountain water resources: overview and recommendations for research, management and policy, Hydrol. Earth Syst. Sci., 15, 471–504, doi:10.5194/hess-15-471-2011, 2011.

Veatch, W., Brooks, P. D., Gustafson, J. R., and Molotch, N. P.: Quantifying the effects of forest canopy cover on net snow accumulation at a continental, mid-latitude site, Ecohydrology, 2, 115–128, 2009.

Washichak J. N. and McAndrew, D. W.: Snow Measurement Accuracy in High Density Snow Course Network in Colorado, Proceedings of the 35th Western Snow Conference, Boise, Idaho, USA, April, 1967.

Winstral, A., Elder, K., and Davis, R. E.: Spatial Snow Modeling of Wind-Redistributed Snow Using Terrain-Based Parameters, J. Hydrometeorol., 3, 524–538, 2002.